Check for updates

Key factors for ultra-high on/off ratio thin-film transistors using as-grown carbon nanotube networks†

Yun Sun, ‡[ab] Pengpeng Li, ‡[ab] Esko I. Kauppinen,[c] Dong-Ming Sun ⓘ *[ab] and Yutaka Ohno*[d]

Approximately 30% of as-grown carbon nanotube (CNT) networks are metallic, usually leading to a trade-off between carrier mobility and on/off ratio in CNT thin-film transistors (TFTs). Figuring out the key factors of ultra-high on/off ratio in CNT TFTs should be considerably essential for the development of large-scale electronic devices in the future. Here ultra-high on/off ratios of 10^7–10^8 are realized for CNT TFTs with mobility of ~500 cm^2 V^{-1} s^{-1}. We propose that one of the key factors to achieve the high on/off ratio is a clean CNT thin film without charge traps and doping due to residual dispersant used in conventional solution processes. Moreover, on/off ratio degradation under operation voltage is significantly suppressed by decreasing the diameter of CNTs.

Introduction

Networks of single-walled carbon nanotubes (CNTs) have attracted much attention as an active layer in thin-film transistors (TFTs).[1] Such a thin-film material exhibits uniform properties by averaging properties of individual CNTs, providing a route to practical uses of CNT-based electronics systems. The CNT TFTs are expected to enable a fabrication of high-performance integrated circuits for flexible and transparent devices on a plastic film, using relatively simple techniques such as solution,[2,3] printing,[4] and sheet transfer processes.[5–7]

One of the important issues of CNT TFTs to be addressed is to improve the on/off ratio. As-grown CNT networks usually contain metallic CNTs of 30%, which lead to a trade-off between carrier mobility and on/off ratio in CNT TFTs.[1,8] Many techniques have been developed to eliminate the drawbacks of metallic nanotubes,[9–14] for instance, solution-processed techniques, such as density gradient ultracentrifugation (DGU)[15] and gel filtration technique,[16] are representative to separate

metallic and semiconducting CNTs effectively. Nowadays, the purity of semiconducting CNTs above 99% have been achieved with the help of state-of-the-art polymer-sorted DGU,[17–20] and the resultant CNT TFTs exhibit on/off ratio around 10^8 with mobility of 297 cm^2 V^{-1} s^{-1}.[17] But the scalability of solution-processed CNT film should be an inevitable issue for their applications in large-scale flexible electronic devices compared with the meter-scale and roll-to-roll as-grown CNT films,[21] even though the fabrication of CNT TFTs is wafer-scale across 200 mm silicon substrates right now.[22] On the other hand, the selective growth of semiconducting CNTs directly is another route to fabricate high-performance CNT devices,[23] but the poor reproducibility and rigorous synthesis condition would be dealt with urgently in the future. Therefore, figuring out the key factors about improving the on/off ratio in TFTs using as-grown CNT networks could be helpful and prospective for the development of large-scale CNT-based electronic devices in the future.

In the previous work,[7] we reported a gas-phase filtration and transfer process to fabricate the CNT TFTs exhibiting the carrier mobility of 634 cm^2 V^{-1} s^{-1} and the on/off ratio of 6×10^6. Here using the devices with high on/off ratio, we investigate the causes of degradations of on/off ratio of CNT TFTs for various cases, such as the residual dispersant, chemical doping and CNT diameter. Then through the systematic characterization and analysis, we clarify that key factors to realize ultra-high on/off ratios in CNT TFTs should be a clean CNT thin film without charge traps and doping. In addition, CNTs with smaller diameters are quite competent for restraining the on/off degradation under operation voltage. Finally, CNT TFTs with on/off ratio around 10^8 are realized with the mobility of ~500

[a]Shenyang National Laboratory for Materials Science, Institute of Metal Research, Chinese Academy of Sciences, 72 Wenhua Road, Shenyang, 110016, China. E-mail: dmsun@imr.ac.cn

[b]School of Material Science and Engineering, University of Science and Technology of China, 72 Wenhua Road, Shenyang, 110016, China

[c]Department of Applied Physics, Aalto University School of Science, PO Box 15100, FI-00076 Aalto Espoo, Finland

[d]Department of Quantum Engineering, Nagoya University, Furo-cho, Chikusa-ku, Nagoya 464-8603, Japan. E-mail: yohno@nuee.nagoya-u.ac.jp

† Electronic supplementary information (ESI) available. See https://doi.org/10.1039/d2ra02088b

‡ These authors were equal major contributors to this work.

cm^2 V^{-1} s^{-1} simultaneously, providing a bright path for the fabrication of high-performance CNT electronic devices.

Results and discussion

The back-gate CNT TFTs used in this study were fabricated on a p^+-Si substrate with a thermally-oxidized SiO_2 layer of a thickness of 100 nm, by a gas-phase filtration and transfer process. The details of growth and fabrication process have been reported in ref. 7. Fig. 1 shows transfer characteristics of a typical CNT TFT fabricated by the gas-phase filtration and transfer process. The device showed p-type characteristics with the on/off ratio of 5×10^8 and mobility of 496 cm^2 V^{-1} s^{-1} evaluated at the linear region by a rigorous model (ESI S1†).[24] The CNT TFTs simultaneously show both a high mobility and a high on/off ratio. In the previous report,[7] we clarified that the high mobility originated from the unique morphology of the CNT network, that is, the network of long CNTs connected by Y-junctions, by which the number of inter-CNT junctions along

Fig. 1 Typical transfer characteristics (I_D–V_{GS}) of CNT TFTs. The channel length (L_{ch}) and channel width (W_{ch}) are both 100 μm, the thickness of dielectric layer (SiO_2) is 100 nm. The on/off ratio decreases from 5×10^8 to 2×10^7 with $|V_{DS}|$ increasing from 0.5 to 5 V.

the current flow paths and the junction resistances were reduced. At a larger source-drain voltage ($V_{DS} = -5$ V), the minority electron current slightly increases at off state, resulting in a degradation of the on/off ratio.

On/off ratios of CNT TFTs fabricated by different techniques are summarized in Table 1. The typical on/off ratios of the TFTs in this work are between 10^6 and 10^8 at $V_{DS} = -0.5$ V, even though the on/off ratio decreased by one to two orders of magnitude at $V_{DS} = -5$ V, which is still smaller than those reported in the previous literature.[4–6,15] It should be noted that the on/off ratio of CNT TFTs depends on the drain bias because the off current increases with the drain field due to the minority carrier injection from the drain electrode, and that the on/off ratio should be considered at a drain bias under a realistic operation condition. The degradation of on/off ratio under the operation condition seriously increases power consumption of the circuits, such as logic large-scale integrated circuits (LSIs) and active matrices of flat-panel displays. Therefore, how on/off ratio depends on the fabrication technique and drain bias voltage should be comprehended thoroughly.

First, we studied the cause of low on/off ratio of solution-based CNT TFTs. In the solution process, surfactants such as sodium-dodecyl-sulfate (SDS) and sodium-cholate are used to disperse and stabilize CNTs in water.[25,26] However, it is difficult to remove such surfactants completely from CNTs after the device fabrication. In this study, we investigate the effect of surfactant by soaking CNT TFTs in 1% water solution of SDS. Fig. 2a shows transfer characteristics of a CNT TFT before and after soaking in the SDS solution. The on/off ratio decreased from 3×10^6 to 4×10^2. The threshold voltage shifted towards positive V_{GS}, from -5 V to -1 V, this means that the SDS has an ability to dope positive carriers, *i.e.* holes, in CNTs. Such doping effect of SDS has been also observed by XPS and Raman spectroscopy, exhibiting the electron-withdrawing sulfate group as a strong p-dopant.[27] Moreover, the subthreshold slope (s-factor) increased from 0.35 V dec^{-1} to 1.2 V dec^{-1} indicating the charge trapping effect of SDS molecules. The effective trap density per area is estimated as 3.59×10^{11} cm^{-2} eV^{-1} (ESI S2†). The mechanism of the degradation of on/off ratio due to the charge trapping effect is schematically shown in Fig. 2b. Under an
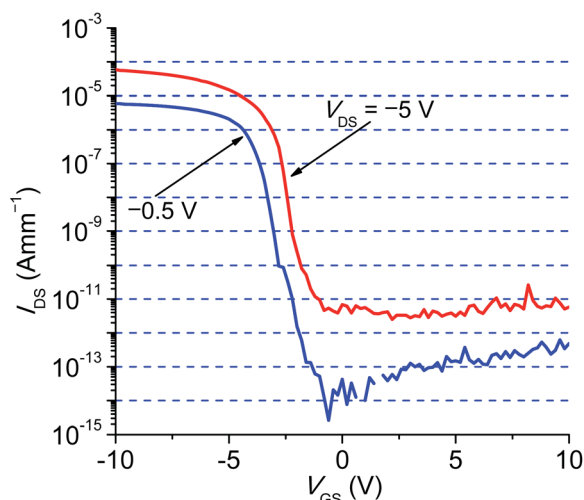
Table 1 On/off ratio degradation of the various CNT TFTs. The CNT TFTs fabricated by a dry process (this work) exhibit much higher on/off ratios than those fabricated by a solution process (Ha *et al.*,[4] Engel *et al.*[15]). For the on/off ratio degradation under a large V_{DS}, the degradation magnitude of the smaller-diameter (1.1 nm) CNT TFTs was obviously improved compared to that of the larger-diameter (1.4 nm, 1.5 nm, 1.3–1.7 nm, 1.6 nm) CNT TFTs

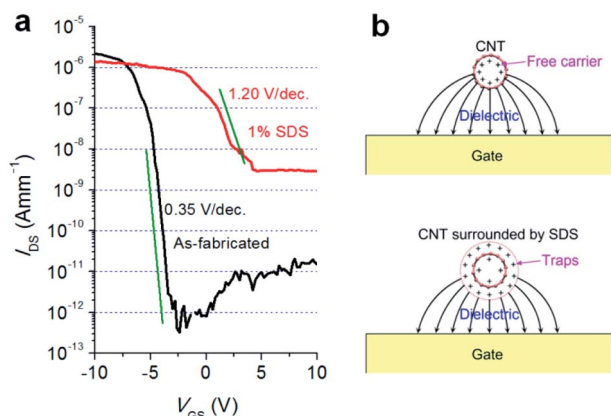| Reference	Low V_{DS}		High V_{DS}		Diameter of CNTs (nm)	CNT synthesis	TFT fabrication
	V_{DS} (V) (average drain field (V m^{-1}))	On/off	V_{DS} (V) (average drain field (V m^{-1}))	On/off			
This work (1.1 nm)	-0.5 (5×10^3)	10^6–10^8	-5 (5×10^4)	10^5–10^7	1.1	Floating-catalyst CVD	Dry process
This work (1.6 nm)	-0.5 (5×10^3)	10^6–10^8	-5 (5×10^4)	10^3–10^6	1.6	Floating-catalyst CVD	Dry process
Cao *et al.*[5]	-0.5 (5×10^3)	∼10^4	-5 (5×10^4)	80	∼1.5	Supported-catalyst CVD	Dry transfer, CNT strips
Ha *et al.*[4]	-0.1 (2×10^3)	∼10^5	-1 (2×10^4)	400	∼1.4	Arc discharge	Solution, DGU
Engel *et al.*[15]	-0.1 (5×10^4)	10^4	-3 (1.5×10^6)	300	1.3–1.7	Arc discharge	Solution, DGU

Fig. 2 Charge trapping effect of the SDS solution on the CNT TFT. (a) On/off ratio degraded from 3×10^6 to 4×10^2 after 1% SDS solution treatment. (b) Schematics of the charge trapping effect of the SDS solution.

existence of traps around the CNTs, charges are captured by the traps with increasing V_{GS}, so that the modulation effect of V_{GS} is restricted. Consequently, the TFTs exhibiting the poor V_{GS} dependence cannot be turned on or off completely, and the on/off ratio decreases. This phenomenon has been often observed in I_D–V_{GS} characteristics of solution-based TFTs.[28–31] The decrease in the on/off ratio can be related to both the carrier doping and the charge trapping effects.

As a matter of fact, when the concentration of surfactants increase, more traps will be introduced and surround CNTs, while more charge carriers will be captured by these traps with the increased V_{GS} leading to the more serious restriction of gate modulation. Similarly, when the ion size of surfactants increase, the capability of capturing charge carriers for one trap will be also enhanced, leading to the increased amounts of trapped charge carriers in all traps.

We investigate the effect of chemical doping on the on/off ratio of CNT TFTs. Fig. 3a shows the change in transfer characteristics by the chemical doping on the CNT TFTs. The
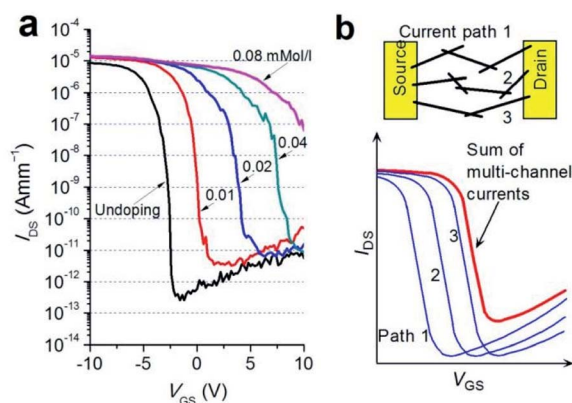
chemical doping was carried out by spin coating of the toluene solution of tetrafluorotetracyano-*p*-quinodimethane (F$_4$TCNQ), which is a p-type dopant for CNTs on CNT TFTs.[29,32] With increasing the concentration of F$_4$TCNQ, the on/off ratio decreased, and the threshold voltage shifted toward the direction of positive V_{GS}, similar to the case of SDS treatment. Fig. 3b shows the schematics of the F$_4$TCNQ doping on the CNT TFT. There are a number of current paths in the CNT thin film, and the drain current of the CNT TFT is the sum of the currents of each path. Even though each path has a large on/off ratio, the on/off ratio of total current can be decreased if the threshold voltage is different for each path due to the electron current at the off state. Such a fluctuation of threshold voltage was observed for the single-CNT channel FETs after the chemical doping with F$_4$TCNQ, without significant decrease in on/off ratio (ESI S3†). In the solution-based chemical doping, the dopant molecules would inhomogeneously stick onto the surface of CNTs, so that, the shift of threshold voltage fluctuates. Consequently, the on/off ratio decreases for the multiple current-path transistors such as CNT TFTs, although that of the single-CNT channel FET does not change significantly.

The barrier for the electron injection can be related to the degradation of the on/off ratio at high drain voltage, since the increase in off current is mainly due to the minority electron current as shown in Fig. 1. In the case of semiconducting CNTs, the diameter determines the energy bandgap, and thus the Schottky barrier for an electron between the metallic and semiconducting CNTs as well as the CNTs and metal electrodes.[33–36] It was reported that the CNTs with the diameter of 1.0–2.2 nm are capable of providing a good on/off ratio.[37] However, the on/off ratios decrease 2–3 orders of magnitude under a higher V_{DS} for the CNTs with the diameter of 1.5 nm, 1.4 nm and 1.3–
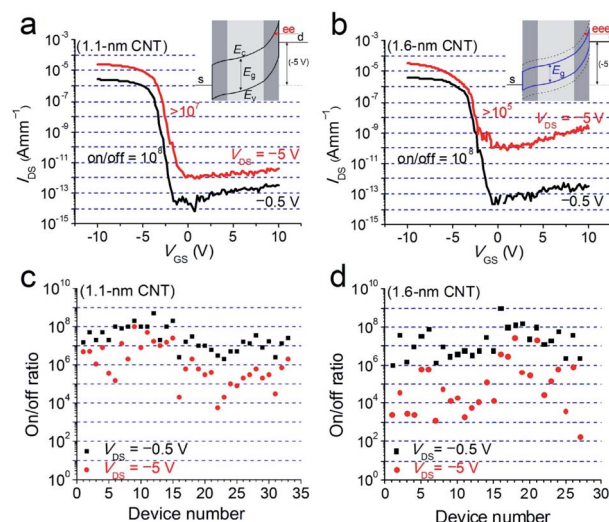

Fig. 3 Chemical doping effect of the F$_4$TCNQ on the CNT TFT. (a) Threshold voltage shifted after the doping of the toluene solution of F$_4$TCNQ with various concentrations. (b) Schematics of chemical doping effect of F$_4$TCNQ.

Fig. 4 Distribution of on/off ratio degradation for the CNT TFTs. (a) and (b) Typical I_D–V_{GS} characteristics of the TFTs, at V_{DS} of −0.5 and −5 V, for the CNTs with diameter of 1.1 and 1.6 nm, respectively. The insets show schematic band diagrams of electron tunneling for 1.1 and 1.6 nm CNTs, respectively. (c) and (d) On/off ratio distributions for 1.1 and 1.6 nm CNTs, respectively.

1.7 nm,[4–6] the on/off ratios of TFTs would be lower than 1000 under practical operation bias, as shown in Table 1.

Fig. 4 shows the on/off ratios of TFTs fabricated by the gas-phase filtration and transfer process for two average diameters of CNTs: (a) 1.1 nm and (b) 1.6 nm. The average diameters were determined from the absorption spectra.[38,39] Both types of CNT TFTs showed similar performance including the carrier mobility and on/off ratio at V_{DS} of −0.5 V. However, the on/off ratios exhibited different degree of degradation at a higher V_{DS} of −5 V. The on/off ratio decreased from 3×10^8 to 2×10^7 for an average CNT diameter of 1.1 nm and from 2×10^8 to 3×10^5 for 1.6 nm. The electron current increased by one order of magnitude for 1.1 nm CNTs and by three orders of magnitude for 1.6 nm CNTs at $V_{DS} = -5$ V. Furthermore, the statistical data regarding the degree of on/off ratio degradation are shown in Fig. 4c and d for 1.1 and 1.6 nm CNTs, respectively. We measured thirty devices for each type of TFTs. For 1.1 nm CNTs, 24% (70%) of devices show the on/off ratio greater than 10^8 (10^7) at $V_{DS} = -0.5$ V, and 19% (60%) of devices greater than 10^8 (10^7) for 1.6 nm CNTs. The on/off ratio degraded 1–2 orders of magnitude for 1.1 nm CNTs, which is much smaller than 2–4 orders for 1.6 nm CNTs. A number of 1.1 nm CNT TFTs exhibited very small on/off ratio degradation (less than 10). This indicates that the on/off ratio degradation phenomenon can significantly be improved by using the smaller-diameter CNTs. Theoretically, the energy bandgap E_g of the semiconducting CNT is inversely proportional to the nanotube diameter d, that is, $E_g = 2\gamma_0 a_{C-C}/d \approx 0.78/d$ (eV), where γ_0 is the tight-binding overlap energy for a carbon–carbon bond and a_{C-C} is the nearest carbon–carbon bond distance.[34,35,40] The energy bandgap value E_g of 1.1 nm and 1.6 nm CNTs are ~0.71 eV and ~0.49 eV, respectively. From the schematic band diagrams as shown in the insets in Fig. 4a and b, it is visible that more electrons can tunnel through the barrier from the drain electrode to semiconducting CNTs, due to the thinner barrier caused by the smaller E_g of 1.6 nm CNT TFT. This leads to the electron current increase and the on/off ratio decrease.

In addition, bundling of CNTs can also degrade the on/off ratio of CNT TFTs because there is an unfavorable electrostatic shielding effect to frustrate gate modulation of the associated semiconducting CNTs if the bundle consists of at least one metallic CNT. The bundle behaves as an electrically metallic wire, leading to reductions in the on/off ratio of TFTs.[41] Therefore, it is preferred to use the individual CNTs rather than thick bundles to form the CNT networks. The networks in the present study consist predominantly of individual nanotubes and a few small bundles, which contributes to the high on/off ratio of TFTs.

Admittedly, the fabrication procedure in this work is similar with the one as described previously,[7] but here we primarily intend to provide a full comprehension and analysis on the key factors that can influence the current on/off ratio of thin-film transistors using as-grown CNT network significantly. Although the fabrication processes and corresponding performance seem to have no significant improvement besides of the post-annealing process, the ultimate goal of these two works are different from each other.

Conclusions

In summary, we realized the high on/off ratios of 10^7–10^9 for the CNT TFTs using a gas-phase filtration and transfer process. The on/off ratio degradation at the high V_{DS} is suppressed with the smaller diameter CNTs. We also investigated the on/off ratio degradation phenomenon by the contaminations from surfactants and chemical doping. In order to realize high on/off ratio, it is well-known to control the density of metallic CNTs lower than the percolation threshold; in this letter, the other two key factors are pointed out: (1) reduce trapping and doping effects by using the clean CNTs as the active layer; (2) select the smaller diameter (~1.1 nm) CNTs to suppress the on/off ratio degradation.

Conflicts of interest

There are no conflicts to declare.

Acknowledgements

References

1 E. S. Snow, J. P. Novak, P. M. Campbell and D. Park, *Appl. Phys. Lett.*, 2003, **82**, 2145–2147.

2 M. C. LeMieux, M. Roberts, S. Barman, Y. W. Jin, J. M. Kim and Z. Bao, *Science*, 2008, **321**, 101–104.

3 C. Wang, J. Zhang and C. Zhou, *ACS Nano*, 2010, **4**, 7123–7132.

4 M. Ha, Y. Xia, A. A. Green, W. Zhang, M. J. Renn, C. H. Kim, M. C. Hersam and C. D. Frisbie, *ACS Nano*, 2010, **4**, 4388–4395.

5 Q. Cao, H. Kim, N. Pimparkar, J. P. Kulkarni, C. Wang, M. Shim, K. Roy, M. A. Alam and J. A. Rogers, *Nature*, 2008, **454**, 495–500.

6 W. J. Yu, S. Y. Lee, S. H. Chae, D. Perello, G. H. Han, M. Yun and Y. H. Lee, *Nano Lett.*, 2011, **11**, 1344–1350.

7 D. M. Sun, M. Y. Timmermans, Y. Tian, A. G. Nasibulin, E. I. Kauppinen, S. Kishimoto, T. Mizutani and Y. Ohno, *Nat. Nanotechnol.*, 2011, **6**, 156–161.

8 C. Kocabas, N. Pimparkar, O. Yesilyurt, S. J. Kang, M. A. Alam and J. A. Rogers, *Nano Lett.*, 2007, **7**, 1195–1202.

9 Y. Li, D. Mann, M. Rolandi, W. Kim, A. Ural, S. Hung, A. Javey, J. Cao, D. Wang, E. Yenilmez, Q. Wang, J. F. Gibbons, Y. Nishi and H. Dai, *Nano Lett.*, 2004, **4**, 317–321.

10 Y. Ono, S. Kishimoto, Y. Ohno and T. Mizutani, *Nanotechnology*, 2010, **21**, 205202.

11 P. G. Collins, M. S. Arnold and Ph. Avouris, *Science*, 2001, **292**, 706–709.

12 Y. Zhang, Y. Zhang, X. Xian, J. Zhang and Z. Liu, *J. Phys. Chem. C*, 2008, **112**, 3849–3856.

13 L. M. Gomez, A. Kumar, Y. Zhang, K. Ryu, A. Badmaev and C. Zhou, *Nano Lett.*, 2009, **9**, 3592–3598.

14 L. An, Q. Fu, C. Lu and J. Liu, *J. Am. Chem. Soc.*, 2004, **126**, 10520–10521.

15 M. Engel, J. P. Small, M Steiner, M Freitag, A. A. Green, M. C. Hersam and Ph Avouris, *ACS Nano*, 2008, **2**, 2445–2452.

16 T. Tanaka, H. Jin, Y. Miyata and H. Kataura, *Appl. Phys. Express*, 2008, **1**, 114001.

17 F. Hennrich, W. Li, R. Fischer, S. Lebedkin, R. Krupke and M. M. Kappes, *ACS Nano*, 2016, **10**, 1888–1895.

18 Y. Li, M. Zheng, J. Yao, W. Gong, Y. Li, J. Tang, S. Feng, R. Han, Q. Sui, S. Qiu, L. Kang, H. Jin, D. Sun and Q. Li, *Adv. Funct. Mater.*, 2022, **32**, 2107119.

19 T. Lei, L. L. Shao, Y. Q. Zheng, G. Pitner, G. Fang, C. Zhu, S. Li, R. Beausoleil, H.-S. P. Wong, T. C. Huang, K. T. Cheng and Z. Bao, *Nat. Commun.*, 2019, **10**, 2161.

20 L. Liu, J. Han, L. Xu, J. Zhou, C. Zhao, S. Ding, H. Shi, M. Xiao, L. Ding, C. Jin, Z. Zhang and L. M. Peng, *Science*, 2020, **368**, 850–856.

21 B. W. Wang, S. Jiang, Q. B. Zhu, Y. Sun, J. Luan, P. X. Hou, S. Qiu, Q. W. Li, C. Liu, D. M. Sun and H. M. Cheng, *Adv. Mater.*, 2018, **30**, 1802057.

22 M. D. Bishop, G. Hilles, T. Srimani, C. Lau, D. Murphy, S. Fuller, J. Humes, A. Ratkovich, M. Nelson and M. M. Shulaker, *Nat. Electron.*, 2020, **3**, 492–501.

23 Z. Zhu, N. Wei, W. Cheng, B. Shen, S. Sun, J. Gao, Q. Wen, R. Zhang, J. Xu, Y. Wang and F. Wei, *Nat. Commun.*, 2019, **10**, 4467.

24 Q. Cao, M. Xia, C. Kocabas, M. Shim and J. A. Rogers, *Appl. Phys. Lett.*, 2007, **90**, 023516.

25 M. J. O'Connell, S. M. Bachilo, C. B. Huffman, V. C. Moore, M. S. Strano, E. H. Haroz, K. L. Rialon, P. J. Boul, W. H. Noon, C. Kittrell, J. Ma, R. H. Hauge, R. B. Weisman and R. E. Smalley, *Science*, 2002, **297**, 593–596.

26 N. R. Tummala and A. Striolo, *ACS Nano*, 2009, **3**, 595–602.

27 K. R. Moonoosawmy and P. Kruse, *J. Am. Chem. Soc.*, 2010, **132**, 1572–1577.

28 Y. Miyata, K. Shiozawa, Y. Asada, Y. Ohno, R. Kitaura, T. Mizutani and H. Shinohara, *Nano Res.*, 2011, **4**, 963–970.

29 T. Takenobu, T. Kanbara, N. Akima, T. Takahashi, M. Shiraishi, K. Tsukagoshi and H. Kataura, *Adv. Mater.*, 2005, **17**, 2430–2434.

30 Q. Cao, S. H. Hur, Z. T. Zhu, Y. Sun, C. Wang, M. A. Meitl, M. Shim and J. A. Rogers, *Adv. Mater.*, 2006, **18**, 304–309.

31 C. Wang, J. C. Chien, K. Takei, T. Takahashi, J. Nah, A. M. Niknejad and A. Javey, *Nano Lett.*, 2012, **12**, 1527–1533.

32 Y. Nosho, Y. Ohno, S. Kishimoto and T. Mizutani, *Nanotechnology*, 2007, **18**, 415202.

33 R. Saito, G. Dresselhaus and M. S. Dresselhaus, *Physical Properties of Carbon Nanotubes*, Imperial College Press, London, 1998.

34 J. W. Mintmire and C. T. White, *Carbon*, 1995, **33**, 893–902.

35 J. W. G. Wildöer, L. C. Venema, A. G. Rinzler, R. E. Smalley and C. Dekker, *Nature*, 1998, **391**, 59–62.

36 Z. Chen, J. Appenzeller, J. Knoch, Y. Lin and P. Avouris, *Nano Lett.*, 2005, **5**, 1497–1502.

37 S. Salamat, X. Ho, J. A. Rogers and M. A. Alam, *IEEE Trans. Nanotechnol.*, 2011, **10**, 439–444.

38 Y. Tian, M. Y. Timmermans, S. Kivisto, A. G. Nasibulin, Z. Zhu, H. Jiang, O. G. Okhotnikov and E. I. Kauppinen, *Nano Res.*, 2011, **4**, 807–815.

39 Y. Tian, H. Jiang, J. V. Pfaler, Z. Zhu, A. G. Nasibulin, T. Nikitin, B. Aitchison, L. Khriachtchev, D. P. Brown and E. I. Kauppinen, *J. Phys. Chem. Lett.*, 2010, **1**, 1143–1148.

40 Y. Asada, F. Nihey, S. Ohmori, H. Shinohara and T. Saito, *Adv. Mater.*, 2011, **23**, 4631–4635.

41 T. Kim, G. Kim, W. I. Choi, Y. K. Kwon and J. M. Zuo, *Appl. Phys. Lett.*, 2010, **96**, 173107.